Article

Diagnosing the Machine Set Rotor Using Its Relative Vibrations

Piotr Jan Bielawski

Faculty of Marine Engineering, Maritime University of Szczecin, ul. Wały Chrobrego 1-2, 70-500 Szczecin, Poland;
p.bielawski@am.szczecin.pl

Abstract: The efficiency and dependability of machine set depends on the quality of maintenance of functional units of the machine set rotor. Diagnosing the functional units of the machine set can significantly increase the effectiveness and efficiency of the maintenance of the machine set. The purpose of the study was to substantiate the separation of the machine set rotor and demonstrate the possibility of diagnosing such a functional unit using non-contact measurements of its relative vibrations. The measure of the wear margin of the machine set rotor was analyzed, and the symptoms of this measure were examined. Finally, the configuration of the relative vibration sensors of the machine set rotor was investigated. Three models of the relationship between the wear margin measures and the measures of the machine set rotor symptoms were developed for the machine set rotor with a crankshaft supported in slide bearings. One new sensors head (shaft position sensors head) of the relative vibration of the machine set rotor was designed. In each machine set, the rotor of the machine set can be distinguished. The developed models of relationships and designed sensors head can be used as parts of the diagnostic system of the supported slide bearings rotor of the machine set with the crankshaft.

Keywords: machine set rotor; wear margin; relative vibration of the rotor; position sensor head; diagnosing the machine set rotor

1. Introduction

In industrial, transport and energy systems, the machine set as the driving machine-driven machine subsystem can be distinguished. High efficiency and high dependability of such subsystems is in demand in the management of the enterprise asset. The required efficiency and dependability values can be saved and even increased by using appropriate maintenance methods and means, including appropriate diagnostic methods and means.

It is apparent from the available literature that in modern industrial, transport and energy systems, much attention is devoted to the consumption of energy. Models of energy management and energy saving strategies have been created [1,2]. There are many diagnosed objects as well as methods and means of diagnosing an object [3–6]. The terms condition monitoring and diagnostics of machines are in use [7]. Tests with the use of vibration methods are conducted on rotating and non-rotating elements, and methods of vibration measurement are determined in ISO 7919-1 and ISO 10816-1 standards [8,9].

In the literature, the "machine set" is not listed as a diagnosing object. In machine diagnostics, vibration methods have proven their usefulness and are therefore widely used. However, mainly rotating machines are diagnosed. The diagnosis of reciprocating machines with the use of vibration methods is small. According to the author, increasing the quality of maintenance is possible by dividing the diagnosed object into functional units, replacing the concept of condition with the concept of wear margin and creating methods and means of diagnosing a given functional unit [10,11]. The author's earlier research substantiates the thesis that in the machine set, it is advisable to specify the machine set rotor as a functional unit and to comprehensively use relative vibrations as diagnostic symptoms.

The efficiency and dependability of the machine set depends on the energy efficiency and reliability of the functional units of the machine set. The wear margin of each functional

unit is created during the production and assembly. The wear margin is determined by the measure values of features of free and built-in components, operating fluids, movement and load of components in operation. The wear margin becomes exhausted during the use of the machine set due to irreversible wear. Wear intensity is not the same for all functional units of the machine set. The functional unit with exhausted wear margin cannot perform its functions with the required quality or may suddenly fail to operate, which in many cases means the failure of the whole machine set. Therefore, it is necessary to restore the wear margin of the given functional unit in advance. From the economic viewpoint, it is justified to restore the wear margin of only those functional units whose wear margin has been exhausted and for which maintenance will be, to a large extent, separately performed. The information on the wear margin comes from diagnosing a given functional unit.

The basis for diagnosing functional units are diagnostic models describing the relationships between wear margin measures and diagnostic symptoms measures. The aim of the article is to justify the separation of the machine set rotor as a functional unit of the machine set and to demonstrate the possibility of diagnosing such a functional unit by means of non-contact measurements of its relative vibrations. The investigation will focus on the rotor with slide bearing and crankshaft. It is necessary to present a model of machine set rotor, process-dependent forces and moments acting on the rotor, and forces and moments dependent on the wear of the machine set elements. The wear margin measures of radial and axial slide bearings and measures of the machine set rotor shaft alignment should also be demonstrated. Considerations should include diagnostic relationships between the wear margin measures and vibration symptoms, as well as problems related to non-contact measurements of relative vibration of the rotor.

Diagnosing the machine set rotor can significantly increase the effectiveness and efficiency of the machine set maintenance. Diagnostic models of the machine set rotor facilitate the preparation and implementation of diagnostic tests. For the same functional units, the same diagnostic technologies can be used, regardless of the function and design details of the subsystem.

2. Machine Set Rotor, Vibration and Mechanical Efficiency of the Machine Set Rotor

In this paper, it was assumed that:

- machine diagnosing is part of machine maintenance; and
- the relative vibrations of the machine rotor contain diagnostically useful information.

Maintenance-oriented diagnosis can be improved by dividing the machine set into functional units and replacing the term of condition with the term of wear margin. The description of diagnostic relations in real machines is difficult; a sufficiently detailed description is possible on models of machines. In diagnosis, the relationship between the wear margin measure and the symptom measure must be reversible. The algorithm of diagnosing the machine set rotor using its relative vibrations is shown in Figure 1.

A machine set, also referred to as a machine train, is a set consisting of at least one driving machine and one driven machine, while the power transmission to the driven machine is performed by a rotating shaft (Figure 2). Each machine of the machine set has a supported bearing-fixed rotor; each rotor can by modeled as consisting of a disk and a shaft. In the case of sufficiently rigid shafts, the connected rotors form the rotor of a machine set with a specific mass moment of inertia θ (kg·m^2), rotary (angular) speed ω (rad/s) and kinetic energy $E_{kin} = \theta \cdot \omega^2 / 2$. The driving machine rotor disk is affected by a driving moment, while the rotor disk of the driven machine is affected by the driven, i.e., effective, moment. In machine set rotor supports the existing motion resistance, generates a moment of friction.
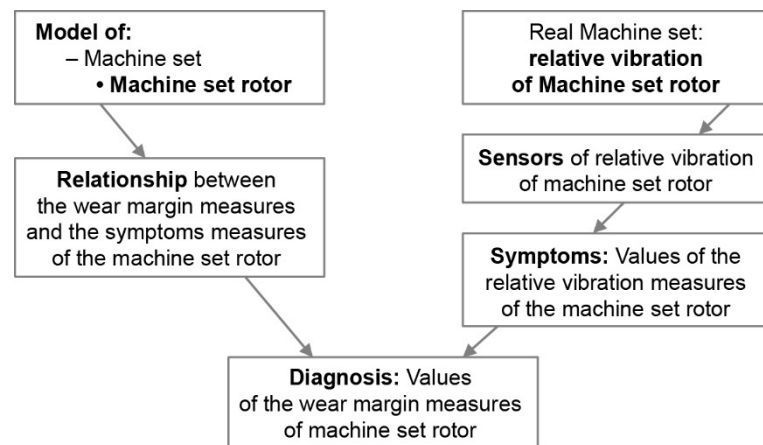
Figure 1. The algorithm of diagnosing the machine set rotor using its relative vibrations.
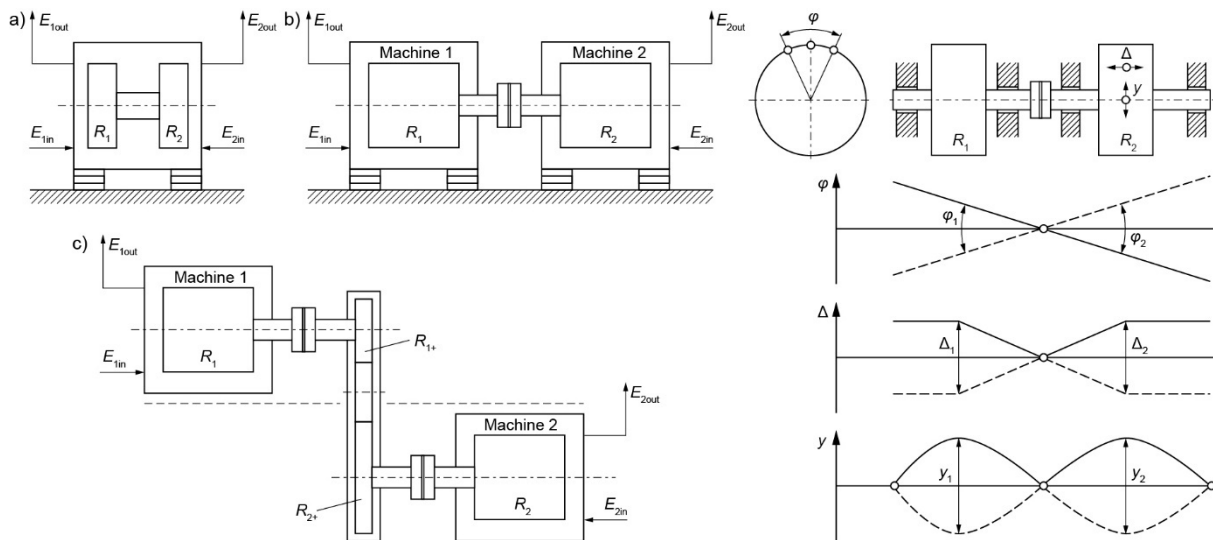

Figure 2. Rotors of the driving machine-driven machine set (on the left) and vibrations of the two-mass machine set rotor (on the right): (**a**) one rotor with one shaft, (**b**) one rotor with shafts connected by a coupling, (**c**) two rotors of a machine set with a transmission, E_{1in}—energy powering the driving machine, E_{1out}—energy carried away from the driving machine, E_{2in}—energy delivered to the driven machine, E_{2out}—energy at driven machine output, R_1—rotor disc of the driving machine, R_2—rotor disc of the driven machine, R_{1+}, R_{2+}—rotor discs of the transmission, φ—angular displacement of torsional vibration, Δ—displacement of axial vibrations, y—displacement of radial vibration.

The functional unit specified in this article, called a "machine set rotor", has a shaft made in one piece (Figure 2a) or a shaft consisting of two shafts connected by a coupling (Figure 2b). Where two machines are connected through a transmission (Figure 2c), two rotors of a machine set are distinguished: one is a rotor of the driving machine and a rotor of the first transmission shaft; the other is the last rotor of the transmission and the rotor of the driven machine. Other elements can be placed between the coupling discs of the machines: intermediate shaft, flexible coupling, a clutch or others. Both single machines of a machine set may have more than one rotor.

The machine set rotor can be modeled as at least two masses connected by a massless shaft with specific rigidity and damping. The two-mass rotor has one node in the case of torsional and longitudinal vibration and three nodes in the case of the second mode radial vibrations (Figure 2). In the nodes, the values of vibration of a given type are equal to zero and increase along with the distance from the node. All vibrations of the machine set rotor are damped. Damping takes place in the shaft material and in the rotor bearings (viscosity

damping). If the forces or moments acting on the rotor are periodic forces, then resonance vibrations may occur. The periodic forces can be decomposed into harmonic components.

One of the characteristics of the driving-driven machine set common in use is the energy efficiency of the set.

In terms of energy, the measure of the wear margin of the machine set is its mechanical energy efficiency or the moment of friction. In the case of rotating machines, the mechanical energy efficiency is equal to the mechanical energy efficiency of the machine set rotor. The mechanical efficiency of the machine set rotor $\eta_{m.MSR}$ can be written as

$$\eta_{m.MSR} = \Delta E_2 / \Delta E_1 = (E_{2\text{in}} - E_{2\text{out}})/(E_{1\text{out}} - E_{1\text{in}}) = (M_U \cdot \alpha)/(M_N \cdot \alpha) \tag{1}$$

where: *MN*—driving moment, *MU*—effective moment, α—angle of shaft rotation [rad].

Moments of friction M_R created in the bearings depend on radial and axial forces acting on the shaft and friction coefficients. The driving moment is equal to the sum of the effective moment and the moment of friction.

$$M_N = M_U + M_R \tag{2}$$

$$\eta_{m.MSR} = M_U / M_N = (M_N - M_R)/M_N = 1 - M_R/M_N \tag{3}$$

If the value of one of the moments is dependent on the rotation angle α of the rotor, then the rotors in the torsional vibration node will experience an instantaneous change of rotor speed $\omega = d\alpha/dt = \dot\alpha$ and, consequently, the kinetic energy of the rotor will change. The power balance and change of kinetic energy can then be written [12,13] as

$$M_N \cdot \dot\alpha - M_u \cdot \dot\alpha - M_R \cdot \dot\alpha = dE_{\text{kin}}/dt \tag{4}$$

$$
\begin{aligned}
dE_{\text{kin}}/dt &= d\left(0.5\theta \cdot \dot\alpha^2\right)/dt = 0.5\left(\dot\alpha^2 \cdot d\theta/dt + 2\theta \cdot d\dot\alpha/dt\right) = \\
&= 0.5 \cdot (d\theta/dt) \cdot \dot\alpha^2 + \theta \cdot \dot\alpha \cdot \ddot\alpha = 0.5 \cdot (d\theta/d\alpha) \cdot (d\alpha/dt) \cdot \dot\alpha^2 + \theta \cdot \dot\alpha \cdot \ddot\alpha
\end{aligned}
\tag{5}
$$

After substitution and dividing by $\dot\alpha = d\alpha/dt$, we obtain the balance of moments, i.e., the equation of the moments of the machine set rotor

$$M_N - M_u - M_R = 0.5 \cdot (d\theta/d\alpha) \cdot \dot\alpha^2 + \theta \cdot \ddot\alpha \tag{6}$$

For $\dot\alpha_{\text{average}} = \text{const}$, $\ddot\alpha_{\text{average}} = 0$, the moments of forces and the moment of inertia can have instantaneous values dependent on the rotor rotation angle. For a given machine set rotor, variations of $d\theta/d\alpha$ are known. $d\theta/d\alpha \neq 0$ mainly refers to piston machines and is determined at the design stage, and the period of changes is one revolution of the crankshaft.

For the rotor of the rotating machine set $d\theta/d\alpha = 0$, the value of the product $\theta \cdot \ddot\alpha$ with respect to the rotation angle is the sum values of the other components of the equation of moments. The values of the driving and effective moments as a function of the rotation angle are specific to the given type of machine.

Equation (6) can be seen as one of the relationships between the wear margin measure given as the friction moment and the symptom measure of the machine set rotor given as the angular acceleration of torsional vibrations.

If direct and precise measurements of the angular acceleration in the torsional vibration node of a machine set rotor were feasible, two specific forms of diagnosis would be available:

1. In these working states, the driven machine can be in the working mode $M_U > 0$ or run idle, without a load, $M_U = 0$. For a constant average angular speed, the value of the components of Equation (6) with respect to time can be considered as periodic signals, and each of them can be presented as the sum of harmonic signals with specific values of the harmonic order, amplitude and phase angle. It is possible to determine the reference spectrum of the driving moment and effective moment. Additionally, the

reference spectrum of the friction moment can be determined. It can be assumed that for a given machine set rotor and for a specific average rotary speed, there exists a model of value as a function of the rotation angle and a spectrum model of the angular acceleration $\ddot{\alpha}$. Comparing the real value as a function of the rotating angle or real spectrum with their respective models, we can draw conclusions on the changes in the moments of a machine set.

2. In tests of average acceleration during runup ($M_N > 0$, $\ddot{\alpha}_{\text{average}} = \varepsilon_r > 0$) and rundown ($M_N = 0$, $\ddot{\alpha}_{\text{average}} = \varepsilon_w < 0$) without external load, it is possible to determine the mechanical efficiency of the machine set rotor $\eta_{m.a\,x}$ for a selected speed ω_x [14–17].

$$\eta_{m.a\,x} = \varepsilon_{r\,x}/(\varepsilon_{r\,x} - \varepsilon_{w\,x}) \tag{7}$$

Damage to the rotor elements may result in the rotor natural frequency drift and the change of vibration node positions, e.g., Ref. [18]. The angular acceleration outside the torsional vibration node contains components depending on the value of the torsional vibration acceleration at the point of observation. In such causes, in Equations (6) and (7), the average value of angular acceleration must be used.

3. Qualities and Symptoms of the Wear Margin of the Machine Set Rotor

3.1. Quality of the Machine Set Rotor Wear Margin

The wear margin of the machine set rotor as a functional unit created conceptually for diagnostic purposes is not determined in the specifications of machines. Therefore, for diagnostic purposes, appropriate quality and quality measures should be indicated for the machine set rotor wear margin and associated with appropriate measures of diagnostic symptoms. Wear margin quality measures can be different for machine set rotors supported in rolling bearings, slide bearings and for machine set rotor with a crankshaft.

Generally, if the wear margin of the machine set rotor has a nominal value, then such rotor will be affected by radial, axial and tangential forces, determined in specifications of the component machines; these forces will be dependent on the current efficiency of the driven machine (or the current load of the driving machine). The wear margin of the machine set rotor can achieve the nominal value if:

- the shaft line axis of the machine set rotor will be a straight line;
- centers of the masses of the machine set rotor will overlap with the rotation axis of the machine set rotor;
- the rotor discs will be permanently connected with the shaft, and the masses and moments of inertia of the rotor discs and the shaft rigidity will conform with the specification.

For real rotors, certain deviations are allowed from the above conditions. The following types of deviation are in use: shaft line alignment [19], rotor unbalance [20] and transfer function [21]. The alignment of the machine set rotor, its unbalance and transfer function should be considered as quality of the wear margin of the machine set rotor. The consequences of incorrect alignment and unbalance of the machine set rotor are additional variable and constant forces acting on the rotor. These contribute to the generation of relative vibrations of the rotor and absolute vibration of bearing support. The values of the generated vibration depend on the transfer function of the machine set rotor and the transfer function of the machine set body [22–24]. The causes of rotor unbalance are described in Refs. [24–26].

The machine set rotor will be properly aligned if:

- rotor components (shafts and discs, including coupling discs) of the machine set will not have errors of shape and position;
- there will be no coaxiality errors of holes for bearings, errors of shape and hole dimensions, errors of shape and dimensions of shells and rolling bearings;
- support bearings will have oil film of proper thickness.

Errors in couplings connecting the rotors of machines in a set consist of manufacturing and assembly errors and the wear of the couplings. In Ref. [27], the types of coupling errors are distinguished.

Non-coaxiality of the support bearings leads to changes in the values of the reaction forces in the bearings and the deformation of the machine set rotor shaft. Additional constant reaction forces in the bearings are created, and the shaft is additionally bent. Consequently, the bearings become overloaded, and stresses in the shaft lead to fatigue damage. The possible causes of bearing non-coaxiality are:

(a)　alignment errors—a typical alignment error leads to a constant (non-rotating) bending line of the shaft centerline [27]. Journals are displaced, particularly the first journals on the coupling side, mainly slide bearings (displacement within the bearing clearance). These deviations, referred to as angular offset and parallel offset, are measurable on the disconnected shafts of the machine set rotor.

(b)　displacement of the shaft bearing support of one of the machines. The displacement of bearing support may be caused by deformations of the support, machine body or foundation. Deformations of machine foundations are specific for a given production system and, in many cases, are given in the system specification. For instance, deformed foundation can be due to deformations of the ship's hull [19]. The causes of support displacement are described in Ref. [28].

Machine specification often determines the allowable values of the dimension and shape deviations, referring to both holes for bearings and to the shell. Incorrect holes for bearings may be caused by incorrect manufacturing, incorrect assembly of the covers and the connecting bolts or wear of the hole surface. It provides poor connection of the bearing (shell, roller bearing) with the bearing support/machine body. Consequently, fretting corrosion may develop. Fretting corrosion causes the oil film temperature to increase and the viscosity and film thickness to decrease, etc.

The thickness of oil film in the bearing depends on the wear margin of a given bearing (see Section 3.2). The loss of wear margin (loss of bearing capacity) of slide bearings is usually the consequence of lubricating oil deterioration and the wear of the journal and shell material. The loss of wear margin will occur if the wear causes, e.g., the diameter of bearing elements to decrease, e.g., the journal diameter by 0.02 mm, shell thickness by 0.05 mm [29]. One consequence of lost wear margin in a radial bearing is radial displacement of the journal in the shell. The radial displacement of the journal relative to the shell may result in the loss of shaft and sealings concentricity. The eccentricity of the shaft and sealings may result in the loss of shaft sealing tightness.

The alignment of the machine set rotor has direct impact on the reaction forces in the rotor bearings of non-working machines. In many cases, the reaction forces can be measured. The methodology of reaction forces measurement in slide bearings is shown, for instance, in Ref. [30].

3.2. Qualities and Symptoms of the Wear Margin of Machine Rotor Slide Bearings

The machine set rotor can be fixed spatially in radial and axial slide bearings and may, within bearing clearances, move radially and axially. The moment of friction in a slide bearing depends on the friction coefficient. The friction coefficient, a subject of many analyses, is presented in various forms, e.g., as the Stribeck curve [31].

The tribology modeled the slide bearing as two solid bodies with a converging gape filled with fluid. If between the interacting solid bodies (structural elements) a narrow and converging gap exists, filled with fluid, then a pressure is created in the fluid [32]. The pressure in the gap results from the effect of oil wedge and/or extrusion of fluid from the gap. The effect of the oil wedge occurs when the gap walls are convergent (in the geometric sense, i.e., the space between the walls becomes narrower in the direction of the motion), and along the gap, there is a relative speed of the walls $U = w_2 - w_1$, Figure 3 [32,33].
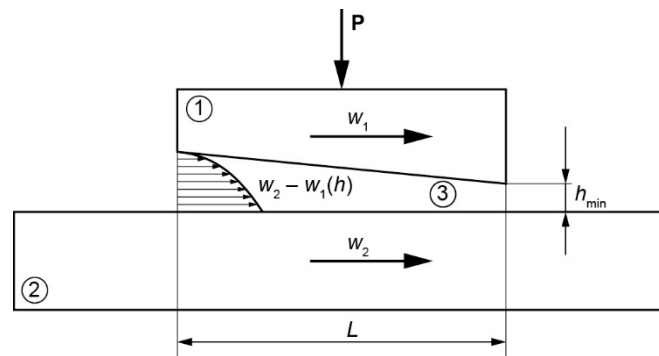
Figure 3. Tribological model of slide bearing. The converging gap and the distribution of fluid speed in the gap: 1, 2—elements forming a node moving at speed w_1 and w_2: $w_2 > w_1$; 3—separating fluid; L—length of the gap; h_{min}—minimum height of the gap; P—normal force exerting a load on the node.

The friction coefficient μ in the convergent gap depends on the "minimum height" of the separating liquid h_{min} and the roughness of the interacting surfaces [34,35].

$$\mu = f\,(h_{min}, R_{az}) \tag{8}$$

$$R_{az} = (R_{a1}{}^2 + R_{a2}{}^2)^{0.5} \tag{9}$$

h_{min}—minimum height of the separating gap (minimum thickness of the oil film),
R_{az}—substitute measure of the surface roughness of the interacting walls,
R_{a1}, R_{a2}—mean arithmetic deviations of the profile from the mean line of walls 1 and 2 forming the tribological node.

The minimum thickness of the separating liquid is proportional to Hersey number H_e [36]

$$H_e = \eta \cdot U / \overline{p} \tag{10}$$

$\overline{p}$—unit load, $\overline{p} = P/(L \cdot B)$, B—gap width,
η—dynamic viscosity of the fluid,
U—slip speed: $U = w_2 - w_1$.

There is a bracket of desired values $h_{min1} < h_{min} < h_{min2}$ for a given bearing:

h_{min1}—the limit relevant to the bearing failure,
h_{min2}—the limit relevant to the loss of energy efficiency.

Table 1 presents the classification of machine set rotor slide bearings.

Table 1. Classification of the machine set rotor slide bearings.

Direction of action of the transferred forces:	radial	axial
Purpose:	supporting	thrust/locating
Method of obtaining the converging gap (wedge):	eccentricity of the journal and the shell axes	- shape (wedge) giving (thrust/locating), - self-aligning bearing segments (Michell bearings)
Design details:	split bearing, sleeve bearing	one-way, two-way, single-acting, double-acting

The methodology of slide bearing design is described in a number of publications, and comprehensive descriptions are found in Refs. [37–41].

For bearings with the convergent lubricating film, the qualities characterizing the load capacity of the bearing have a form of a dimensionless similarity number. The similarity number of slide bearings can be considered as a measure of the bearing wear margin, while the minimum height of the separating gap h_{min} can be considered as the symptom measure of the wear margin. Dependencies between the similarity numbers and the oil

film thickness are described by means of differential equations or diagrams included in the corresponding standards.

For axial bearings (Figure 4), the bearing load capacity is commonly expressed using the number B_k [37,42].

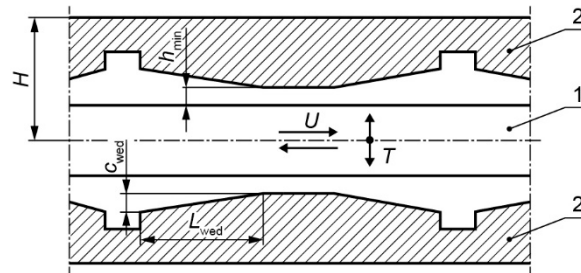$$B_k = \left(\bar{p} \cdot h^2\text{min}\right)/(\eta \cdot U \cdot L) \tag{11}$$

Figure 4. Model of the axial bearings with permanent wedges for work in both directions of force T and speed U: 1—shaft flange, 2—shells attached to the machine body, T—axial force exerting load on the bearing, U—linear speed of a point on the rotating shaft flange, h_{min}—minimum height of the separating gap (minimum thickness of the oil film), L_{wed}—length of the permanent wedge, C_{wed}—height of the permanent wedge.

For a given axial bearing, the number B_k should have a value lying in a specific range interval. In the standards, the number B_k is presented as the function of $h_{\text{min}}/c_{\text{wed}}$.

For the axial bearing, it can be noted that the distance H between the flange center plane or another plane determined on the shaft and the shell base plane depends on the minimum height of the gap h_{min} (Figure 4):

$$h_{\text{min}} = H - H_0 \tag{12}$$

where H_0—value H for the non-working bearing after the shaft flange is pressed to the shell.

If measurements of the distance H were feasible for axial bearings, changes in the distance value could be considered a measure of the bearing's wear margin symptom, whereas B_k could be considered a measure of the bearing's wear margin:

- for a bearing with 100% wear margin, the value of B_k complies with the specification and $B_k = B_{k1}$, whereas the measured values of the H symptom are $H = H_1$, $H_0 = H_{01}$, respectively;
- if $H = H_2$, $H_0 = H_{02}$, then for $(H_2 - H_{02})/C_{\text{wed}}$ from the standard $B_k = B_{k2} \neq B_{k1}$. The change in the value of B_k can be attributable to a change in the value of one or more quantities of which B_k is composed (12);
- if $H_0 = H_2 < H_{01}$, one of the causes is wear resulting in a change in the length of the gap $L = \Sigma L_{\text{wed}}$. If the change in the gap length is the only cause for the change in the value of B_k, then $L_2 = \bar{p}_1 \cdot (H_2 - H_{02})^2 / (\eta_1 \cdot U_1 \cdot B_{k2})$.

To characterize the load capacity of radial bearings, the dimensionless Sommerfeld number is commonly used.

$$S_O = \left(\bar{p} \cdot \psi^2\right)/(\eta \cdot \omega) \tag{13}$$

where
ω—angular speed of the shaft journal,
ψ—relative clearance, $\psi = C/D$,
C—clearance in the bearing, $C = D - d$,
D—shell diameter,
d—journal diameter.

Here are the example values of the clearance in main bearings (flywheel bearings) of the ship's main engine: normal clearance (mm) 0.270–0.374; wear limit (mm) 0.525 [43].

The Sommerfeld number is a similarity criterion of hydrodynamic slide bearings, in which the oil wedge principle is used. When bearings are similar, i.e., have the same relative length b/d and the same shell contact angle and the same Sommerfeld number, their working conditions are similar. They show the same position of the journal in the shell and the same friction coefficient [44]. One measure of the journal position relative to the shell is eccentricity e. There is a relationship between the eccentricity e, clearance in bearing C and minimum height h_{min} of the gap. The dependences of relative eccentricity $\varepsilon = e/(C/2)$ and relative oil film thickness $h^*_{min} = h_{min}/(C/2) = (1 - \varepsilon)$ on the Sommerfeld number So for various b/d are presented in diagrams [45].

The inverse of Sommerfeld number $1/So$ can be the substitute measure of the radial bearing wear margin [46]. The tribological wear of the bearing results in increased clearance and/or decrease in the liquid viscosity. The $1/So$ decreases along with the increase in the clearance and load, and the decrease in viscosity.

Figure 5 presents the position of the journal center in the clearance circle (circle of radius $C/2$) as the function of the rotary or angular speed. At a steady load, the journal, reaching a certain rotary speed, starts to rise toward the shell center. The journal center leaves the circumference of the clearance circle (point 1) and, as the speed increases, moves along path B, similar to a circle. For a determined rotary speed, at a load whose variable component does not exceed the constant component, the journal trajectory is a figure, e.g., circle O with a specific position of the center (point 2) and a specific radius S (Figure 5).
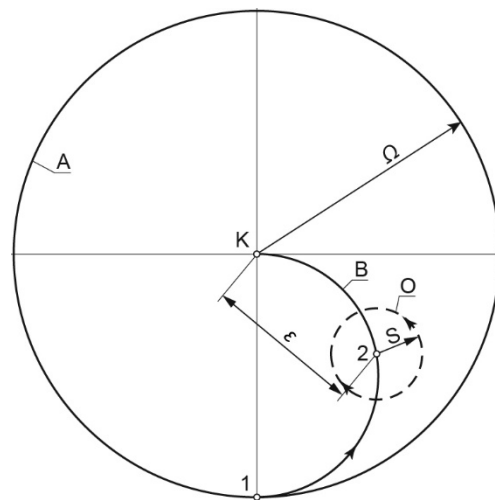

Figure 5. Model of the radial bearing. The trajectory of journal center: Ω—radius of the clearance circle. $\Omega = C/2$; C—clearance in the bearing; A—circumference of clearance circle; B—path of average values of the journal center trajectory; O—path of the variable component of journal center trajectory; 1—position before journal breaks away from the shell: $h^*_{min} = 0$, $\varepsilon = 1$; 2—average value of journal center trajectory for a specific speed: $h^*_{min} > 0$, $\varepsilon < 1$; K—center of the clearance circle: theoretical position of journal center for speed tending to infinity: $h^*_{min} = 1$, $\varepsilon = 0$.

If measurements of eccentricity e were feasible for radial bearings, eccentricity e could be considered a measure of the bearing's wear margin symptom:

- for a bearing with 100% wear margin, the value of So complies with the specification and $So = So_1$, whereas the measured value of the symptom $e = e_1$ for clearance $C = C_1$;
- for a non-operational bearing with the journal in contact with the bearing shell, $e = e_0 = C/2$: $e_{01} = C_1$, $e_{02} = C_2$;
- if the measured $e = e_2 < e_1$, the wear margin is less than 100%. $So = So_2 \neq So_1$, calculated using the standard for $\varepsilon = \varepsilon_2 = e_2/(C_2/2)$. The change in So can be caused by the So constituents other than the clearance (14).

The distance H between the flange center and the shell base of axial bearings can be considered as an average value of the relative displacement of axial vibration, while the

journal-shell center eccentricity e can be considered as an average value of the relative displacement of radial vibration.

3.3. Symptoms of Misalignment of the Machine Set Rotor with a Crankshaft

The machine set may include piston machines. The rotor shaft of a piston machine is a crankshaft, while a crank is part of the crankshaft. The crank has a specific elasticity and can be subject to deflection. The distance between the crank webs may vary depending on the dimensions of the crank, the value of radial force acting on the crankpin and the main journal eccentricity. The measure of distance change between the crank webs is crank deflection, defined as the difference Δa of the distance value a between two positions of the crank in one plane (Figure 6):

- vertical plane $\Delta a_v = a_{\text{TDC}} - a_{\text{BDC}}$ (TDC—top dead center, BDC—bottom dead center);
- horizontal plane $\Delta a_h = a_{\text{SB}} - a_{\text{PS}}$ (SB—starboard side, PS—port side).
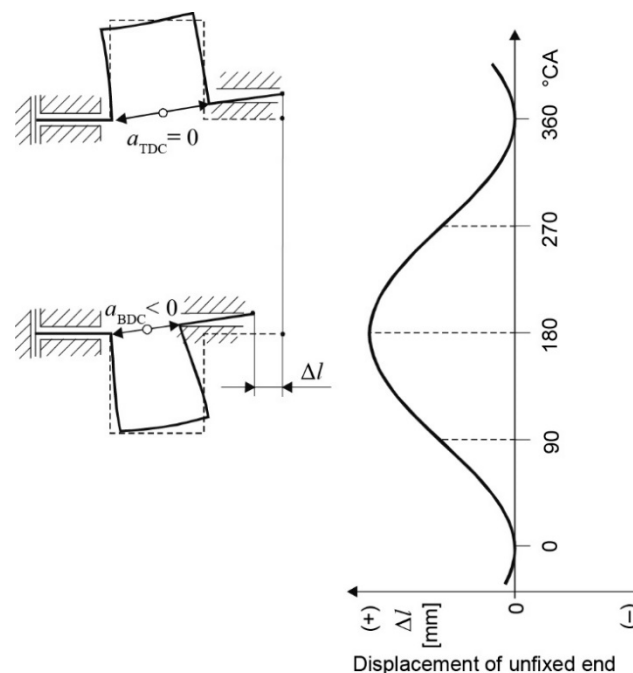

Figure 6. Model of the crank of the unilaterally fixed crankshaft (with one crank) and displacement of unfixed (free) end of crank: Δa—crank deflection; Δl—crank (journal of crank) free end displacements.

The value of distance between crank webs changes as the function of the shaft rotation angle. Variations of the distance are approximately sinusoidal, with the average value equal to $\Delta a/2$ (Figure 6). It can be demonstrated that there is a relationship between shaft alignment and axial vibrations of the shaft free end. For this purpose, performing a thought experiment, we should fix one main journal of each crank, starting from the flywheel end, and sum up the changes of the distances $\Delta l = \Delta a$, accounting for the sign and angular displacement between the cranks. The effect of summing up $\Sigma \Delta l$ is the value of axial displacements of the free end of the crankshaft with respect to the rotation angle [47]. The variations of axial displacement as the function of the rotation angle can be considered as a symptom of crankshaft alignment. The measures of this symptom are amplitude value and phase shift relative to TDC of the first crank and average value [48] (Figure 7). The signal of axial displacement is contained in the axial vibration signal of the shaft free end.
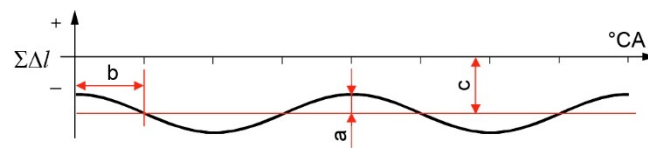
Figure 7. Model of the unilaterally fixed crankshaft. Measures of the crankshaft alignment symptom: a—amplitude, b—phase shift in relation to TDC of first crank, c—mean value.

3.4. Qualities and Symptoms of the Wear Margin of the Machine Set Rotor with a Crankshaft

The fixing of a crankshaft is understood as the impossibility of axial and radial displacement of the first journal center (flywheel side). Because it is impossible to fix the main journal on the flywheel end, the axial and radial positions of that journal center should be measured, and the changes should be taken into account in diagnostic inference. The signal of journal displacement at the flywheel end is contained in the signal of the axial and radial vibrations of that journal.

The axial displacement of the crankshaft free end $\Delta l_{f.e}$ can be measured while the machine is running. The effect of radial forces acting on the crankpin journal is the so-called dynamic deflection of the crank. Like static deflection Δl, dynamic deflection Δl_d is related to axial displacement of the main journals of the cranks and axial vibrations of the shaft ends. The signal of axial vibration of both crankshaft ends is the sum of signals generated by static and dynamic deflection of all the cranks.

If there is only axial displacement $\Delta H(\alpha)$ at the flywheel end, then the axial displacement of the crankshaft free end $\Delta l_{f.e}(\alpha)$

$$\Delta l_{f.e}(\alpha) = \left(\sum_1^n \Delta l(\alpha)\right) + \left(\sum_1^n \Delta l_d(\alpha)\right) - \Delta H(\alpha) \tag{14}$$

where
n—number of cranks,
$\Delta H(\alpha)$—crankshaft displacement at the flywheel end,
α—crankshaft rotation angle.

A change in the eccentricity in the flywheel bearing from e_1 to e_2 causes a change in the value of crank deflection Δa, especially on the first crank, and thus, a change in the value of $(\sum_1^n \Delta l(\alpha))$.

If measurements of the average and instantaneous values and the phase shift of axial vibrations of the free end of the crankshaft $\Delta l_{f.e}(\alpha)$, the average and instantaneous values of axial vibrations of the thrust bearing flange $\Delta H(\alpha)$ and the average and instantaneous values of radial vibrations of the bearing journal at the flywheel end were possible, the quantities could be considered measures of the machine set rotor symptoms:

- if the load is identical and constant on all cranks, the average value, amplitude and phase shift of the axial vibrations of the free end of the crankshaft $\Delta l_{f.e}(\alpha)$ depend on the alignment of the machine set rotor;
- the values of $e(\alpha)$ and $\Delta H(\alpha)$ make it possible to identify the cause of the alignment change. An increase in the eccentricity e in the flywheel bearing indicates non-coaxiality of the set's shafts or wear of the bearing. Changes in the values of ΔH indicate the effect of axial forces from another machine. Where e and ΔH remain constant, a change in the value of vibrations of the shaft free end $\Delta l_{f.e}(\alpha)$ indicates deformations of the support or wear of the bearings supporting the crankshaft.

4. Measurements of Relative Vibration

Measurements of rotating element vibration make use of absolute vibration sensors with a slider or relative vibration sensors (eddy current sensor, inductive or capacitive sensor) [8]. In the case of vibration of rotating elements, diagnosis makes use of relative vibration, mainly radial vibration, in specific cases torsional vibration, and to a limited extent, the axial vibration of the rotating shaft. Relative radial vibration of rotating shafts is

measured in each bearing plane by two sensors, placed at the right angle to each other [8]. Relative axial vibration is used mainly for monitoring the axial shaft position, which consists of monitoring the rotor position relative to a selected constant point, e.g., thrust bearing housing. The measurements are recorded by an axially fixed displacement sensor. For turbomachinery, measurements of absolute axial elongation of the machine body (measured by a sensor on a radial bearing that does not fix the shaft longitudinally) and relative elongation of the body (displacement sensor mounted on the body, monitoring the position of the face or flange of the shaft) are taken [49]. The displacement sensors are usually fixed in holes in non-rotating elements.

It follows from points 2 and 3 of this article that both constant and variable components of the relative vibrations should be measured. Such relative vibration can be measure by common relative vibration sensors placed in the appropriate holder. The holder with the sensor is called here the sensor head.

The vibration of points located on the surface of the selected rotor cross-section is measured relative to or in the plane perpendicular to the rotor axis, called the reference plane. Because the rotor performs all kinds of vibrations simultaneously, the points on the surface of the observed cross-section, apart from the measured motion, also perform other motions, and the reference plane of the measured vibration becomes non-perpendicular to the rotor axis. The problem can be solved by:

- measurements of other types of vibration and correction of the results or;
- measurement of a given type of vibration by more than one sensor and mathematical operations on the measured signals or;
- fixing the reference plane with the rotor axis; the reference plane performs the same motions as the rotor, except for the measured motion.

When vibrations of the same point are measured by a pair of sensors, there will be a phase shift φ between the measured signals depending on the location of the two sensors relative to each other. The measurement results can be recorded in the coordinate system $x(t)$, $y(t)$ or $y(x)$. One of the methods of vibration tests in the $y(x)$ system measured by two sensors shifted by the angle φ are tests using a dual channel oscilloscope working in the XY mode. In the case of vibration with a zero value of the variable ($X_{variable} = 0$, $Y_{variable} = 0$), the result is a point, which for $X = Y \neq 0$ lies on the diagonal of the XY coordinate system.

The interpretation of the obtained image in the XY coordinate system is facilitated by the Lissajous or Bowditch curve. If the vibrations measured by specific sensors were harmonic vibrations with zero average value ($X_{average} = 0$, $Y_{average} = 0$), then their time-dependent variations would be described by the formulae:

$$x(t) = X \sin(\omega_x \cdot t + \varphi), \ y(t) = Y \sin(\omega_y \cdot t) \tag{15}$$

and in the XY coordinate system, they would be figures with a shape dependent on φ, ω_x/ω_y, X/Y. Table 2 presents the Lissajous curves for $\omega_x = \omega_y$, $X = Y$ and the selected angles of phase shift φ.

Table 2. Lissajous curves for $\omega_x = \omega_y$ and $X = Y$.

Phase Shift φ [rad]	0	$\pi/4$	$\pi/2$	$3\pi/4$	π
Figure	/	⬭	◯	⬭	\

The essential element of the time and harmonic analysis of vibration is information on the angular position of the rotor shaft. The harmonic analysis requires the measurement of one rotor rotation period (first harmonic), i.e., time to reach the same angle position. For this purpose, a marker is installed on the rotor, which in the stationary sensor (e.g., optical or inductive) excites one pulse per a single turn. Because the instantaneous angular

position of the selected rotor point depends also on the torsional vibration in the plane of measurement, it is recommended to locate the marker (e.g., key) on the rotor element that rotates at the average, not instantaneous, rotary speed of the shaft. To do this, a converter can be used, consisting of a disc mounted to rotate on the rotor shaft and connected with the rotor by a weak spiral spring (as in the Geiger torsionmeter). According to Ref. [50], a large mass connected with a vibrating object by a weak spring behaves as if it were stationary. Such a converter can be an integral part of the shaft free end head [51].

4.1. Measurements of Torsional Vibration Relative Acceleration of Machine Set Rotors

The acceleration of relative torsional vibration can be measured in each cross-section of the rotor, but in the case of the piston combustion engines, the convenient and practically the only place is the end of the crank shaft. The acceleration of relative torsional vibration can be measured by various heads equipped with various sensors, e.g., tachometric generator, incremental encoder or Ferraris acceleration sensor. The incremental encoder is well known [52]. The principle of the Ferraris sensor was described in Ref. [53]. The advantages and disadvantages of the incremental encoder and the Ferraris acceleration sensor are indicated in Ref. [54].

The head with a Ferraris sensor should have a holder connected with the body, a sensor attached to the holder, and a measuring disc mounted on the rotor, co-operating with the sensor. The measuring disc is made of an electric conductor and generally mounted on a small shaft, an extension of the rotor shaft.

The solution presented in Refs. [51,55] proposes that the Ferraris sensor be mounted rotationally without clearance on the measuring disc shaft and connected with the body by a torsionally rigid element, e.g., bellows coupling.

The tested machine set was composed of a single-crank, three-cylinder piston air compressor driven by electric motor via belt transmission. According to the definition of the machine set rotor given in Section 2, two rotors of the machine set should be distinguished here: the rotor of a compressor with a pulley and the rotor of an electric motor with a pulley. The driving moment produced by the electric motor is not constant during one revolution of the motor rotor. For a bipolar stator, the force acting across the gap between the stator and the rotor is a pulsating force, with a variable component of frequency equal to double frequency of the current in the power supply network [56]. As a result of the slip between the belt and the rotor pulleys, there is a continuous change of phase shift between the motor rotor and the compressor rotor.

Measurements were recorded of the torsional vibration of the compressor free end and phase angles of the compressor and motor rotors. The torsional vibration and phase angle of the compressor rotor was measured by a simplified, workshop-made head described in Ref. [51].

It should be expected that the measured signal of torsional vibration will be the sum of true torsional vibration and the runout signal. The time waveforms of vibration acceleration signals and the angular marker are shown in Figures 8 and 9.
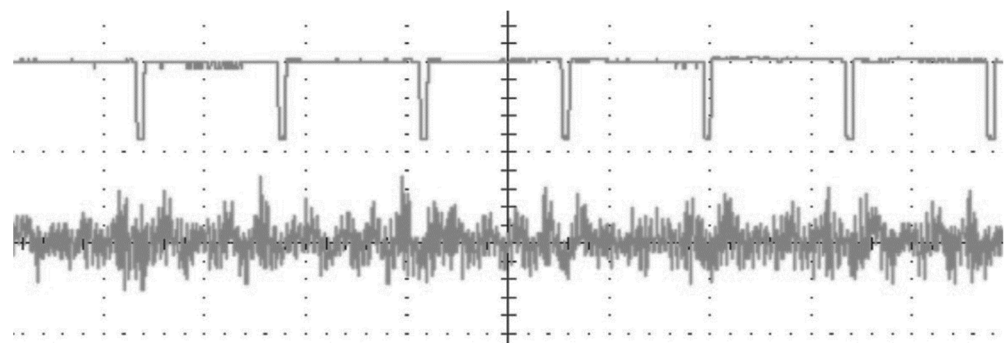

Figure 8. Time waveforms of the signals: upper run—waveform of the compressor shaft marker; bottom run—torsional vibration acceleration of the piston compressor free end.
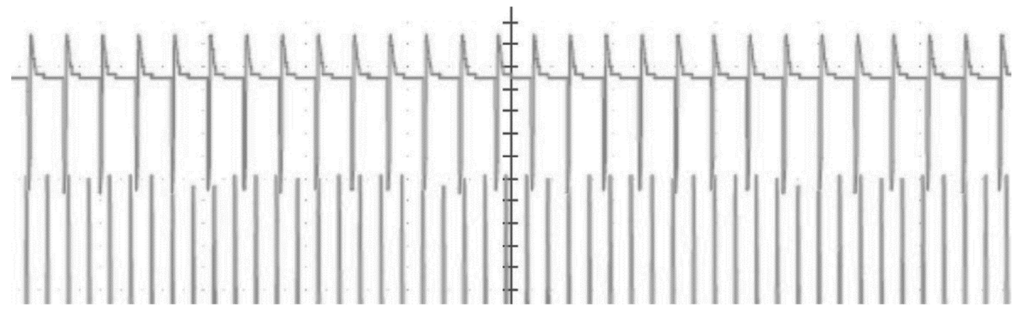
Figure 9. Subsequent periods of the piston compressor shaft and the shaft of the driving electric motor: upper run—signal of the compressor shaft marker; bottom run—signal of the electric motor shaft marker.

The difference was observed in time waveforms of subsequent periods of torsional vibration acceleration of the compressor (Figure 8). It follows from Figure 9 that the period of the compressor rotor is not a multiple of the engine rotor period, and the phase shift between the rotors changes on a continuous basis.

The time waveforms of 16 periods of torsional vibration were subjected to synchronous averaging. The averaged waveform is shown in Figure 10. The synchronously averaged amplitude—frequency spectrum in the 0–500 Hz range was made, Figure 11. Besides, 16 amplitude—harmonic order spectra were synchronously averaged, Figure 12.

Synchronous averaging is a mathematical operation performed on signals to eliminate nonperiodic (random) signals from the periodic signal. Because the value changes of the variable driving moment relative to the changes of effective moment and the friction moment of the compressor are random, synchronous averaging of the signal of the compressor acceleration eliminates, inter alia, the random component of the driving moment.
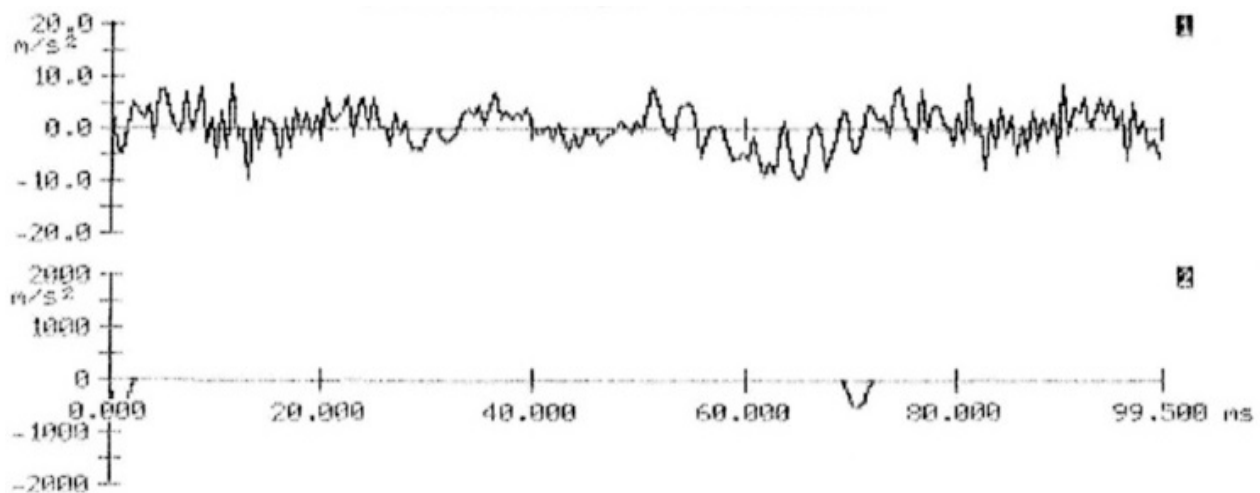

Figure 10. Synchronously averaged waveform of compressor torsional vibration acceleration: high pass filter—1 Hz; low pass filter—1 kHz; 16 averages.
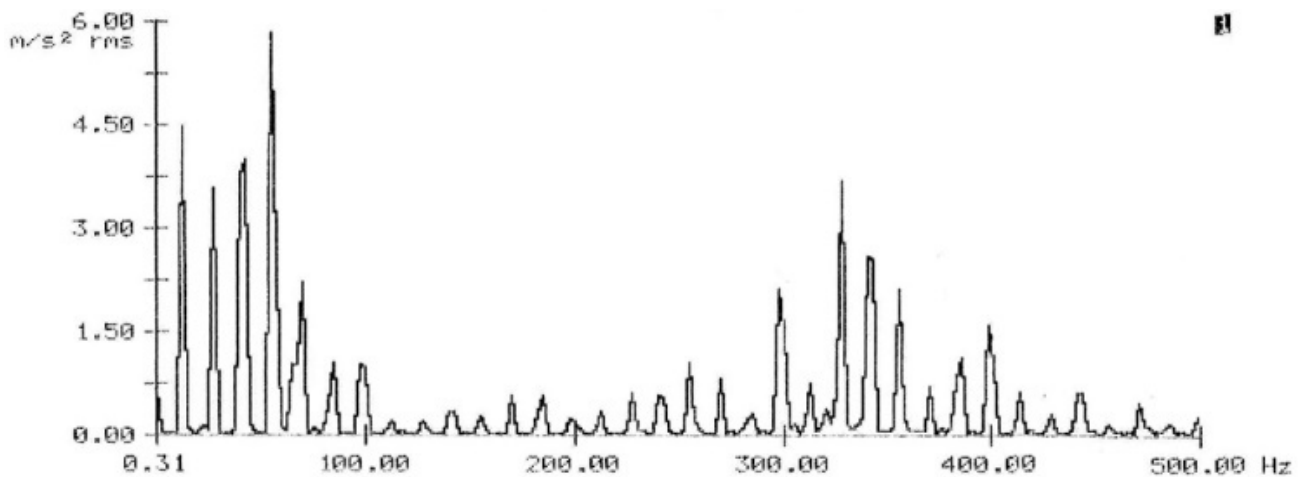
Figure 11. Synchronously averaged spectrum of the torsional vibration acceleration amplitude. Frequency range: 1–500 Hz.
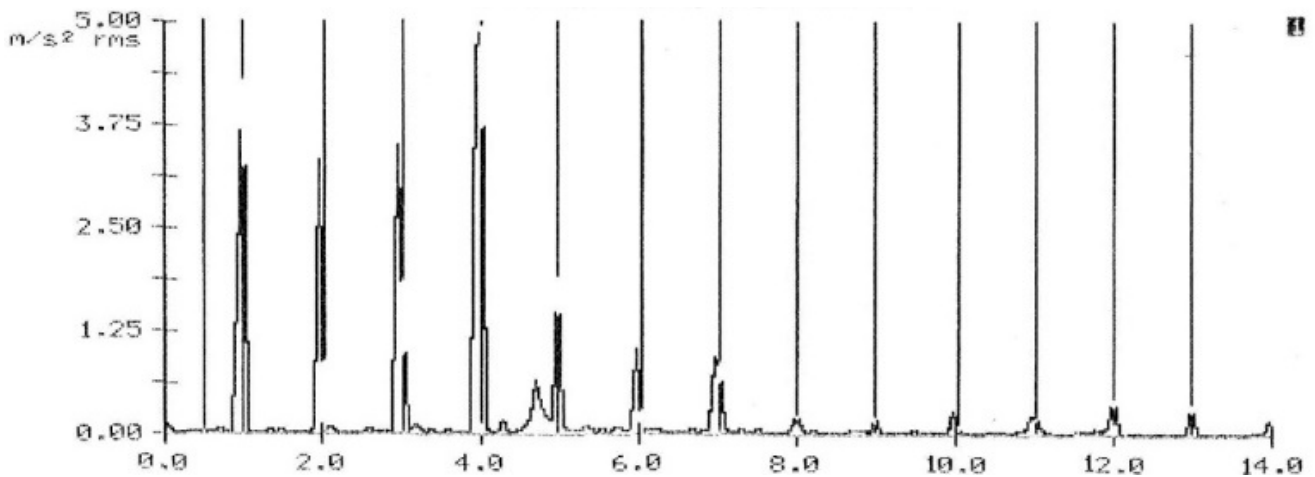

Figure 12. Synchronously averaged spectrum: compressor torsional vibration acceleration. Harmonic order: 1–14 orders.

4.2. Measurements of the Displacement of Rotors' Relative Vibration

The measurement of the relative vibration displacement means that the distance change is measured between the vibration points of the item's element and the point of the reference item, and the measured signal has constant and variable components.

Non-contact sensors of vibration displacement suitable for measurements of relative rotor vibration displacement include the eddy current, inductive and capacitive sensors. Eddy current sensors are characterized by:

- a sufficiently large linear range of the distance-voltage characteristic;
- vibrating element can be made of any electric conductor material, which allows the measurement of vibration without installing additional elements on the rotor.

In the case of eddy current sensors, the distance-voltage characteristic has to be made for a given pair consisting of sensor and vibrating element. Inhomogeneity in the chemical composition of the vibrating material, discontinuities of material macrostructure, errors of shape and position of the vibrating element produce runout signals. The elimination of runout signals requires special procedures, such as processing of journal surface or appropriate processing of the measured signals [57].

4.2.1. Measurements of Journal Eccentricity in the Shell

In the case of radial vibration, the rotor axis is determined by the rotor shaft journal generatrixes. The position of the journal center relative to the shell can be measured in the plane perpendicular to the shaft axis by two displacement sensors X and Y placed at the right angle to each other. In steady-state conditions and a constant load, the trajectory of the journal center in the rectangular coordinate system XY is a point. The load with a variable component results in a plane figure (Lissajous curve) observed in the XY system. The center and radius vector of that figure should be determined. Systems for radial vibration measurement are shown in the standard [10].

The trajectory of the journal center of a radial slide bearing of the rotor kit oil whirl/whip option from Bently Nevada was examined. The rotor was removed and replaced by a shaft, with a diameter inscribed in the shell hole. Eddy current sensors mounted in the shell were set to indicate the same value of voltage. The rotor was mounted again, and the real clearance circle of the bearing was determined by manual rolling of the rotor journal on the inner side of the shell (Figure 13). Then, after engine start-up, the trajectory was recorded at the speed of 2000 rpm (points 2 and 1) and at its change to 260 rpm (Figure 13). The geometric center *K* of the clearance circle was determined (Figure 13). The distance (measured in (V)) between points *K* and 2 and between points K and 1 is the value of absolute eccentricity e_1 at 260 rpm and e_2 at 2000 rpm (Figure 13).
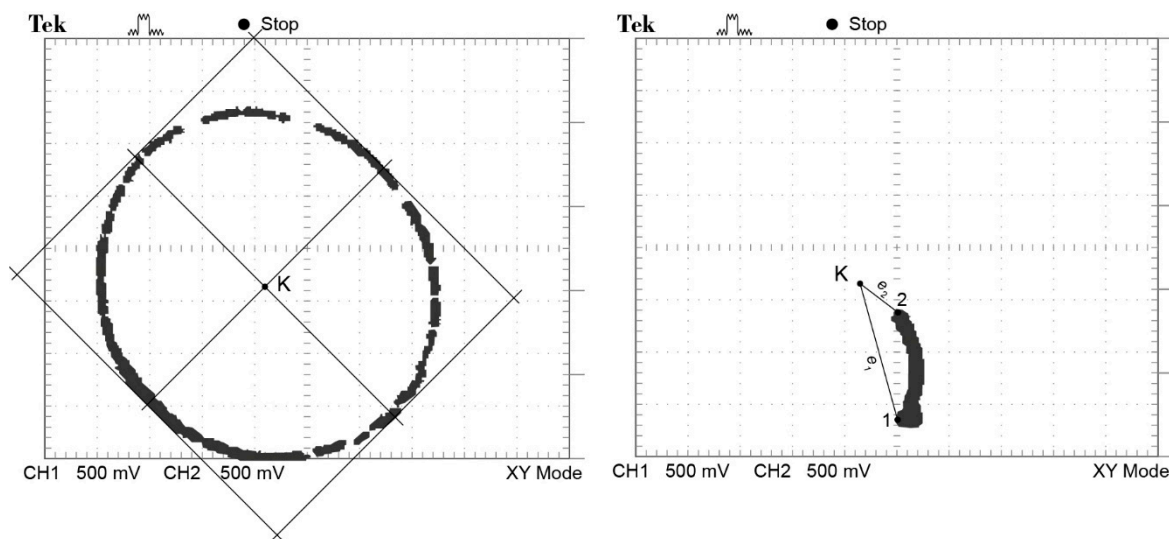

Figure 13. The clearance circle and the trajectory of the journal center at the speed of 2000 rpm and at its change to 260 rpm: K—center of clearance circle, 1—position of journal center for 2000 rpm, 2—position of the journal center for 260 rpm, e_1—value of eccentricity for point 1, e_2—value of eccentricity for point 2.

The standards do not indicate a measurement method for absolute eccentricity of a journal in the shell. To measure the journal-in-shell eccentricity:

- eddy current sensors can be placed in the holder and mounted to the machine body. The sensors in the holder form a measuring head. The sensor axes in the head should be perpendicular to the axis/to the generatrixes of the journal;
- the head on the machine body must be mounted so that the sensor axes intersect with the axis of the shell hole in the machine body;
- the measurement plane should be in a place where the journal is not subject to wear;
- the measuring head must be calibrated, i.e., a specific value of the displacement (displacement signal) measured by the head for the journal located in the center of the shell hole must be specified.

The measuring head cannot be calibrated on the machine to be tested. This can be performed only by using a special auxiliary device—a calibration bushing. The head calibration method for the sleeve bearing is described in Refs [51,58].

4.2.2. Measurements of the Displacement of Relative Axial Vibration

The displacement of axial vibration of a machine rotor can be measured using heads with eddy current sensors attached to the machine body. The head can include (Figure 14):

- one sensor located on the shaft axis; sensor axis is aligned with the rotor shaft axis;
- two sensors with the axes set parallel to the rotor shaft axis, and the same distance of both sensor axes to the shaft axis. The sensors can be mounted circumferentially:
  a. shifted by $\pi/2$,
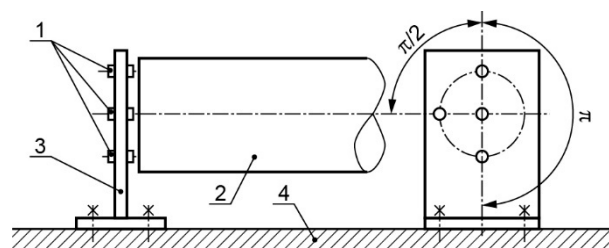 b. shifted by π.

Figure 14. The configuration of sensors of the rotor relative axial vibration: 1—eddy current sensor; 2—rotor shaft; 3—head; 4—machine body.

We should find or place an electric conductor element on the vibrating rotor, with a plane perpendicular to the rotor axis. The surface of this plane cannot be subject to wear. These elements can be as follows:

- face of the rotor shaft free end;
- face of the flange made together with the rotor shaft;
- end face of the flywheel or the face of a special disc mounted on the shaft, etc.

With two sensors, we can analyze the time waveforms $x(t)$ and $y(t)$ from both sensors or images of the value changes in the XY system. The sensors in the head must be set so that they show the same value of axial vibration of the component with the front plane perpendicular to the sensor axis. When a shaft generates only axial harmonic vibration:

- both time waveforms should be identical, have the same average values and should not have a phase shift ($\varphi = 0$);
- in the XY system, the image should be a straight section corresponding to the Lissajous curve for $\varphi = 0$ (Table 2).

The face of the shaft or flange may be positioned non-perpendicularly to the sensors axes and/or have shape errors, and the material under its surface can be inhomogeneous. The measured signals will then contain additional components with a phase angle other than the measured axial vibration. For the most common error, a non-perpendicular shaft face, the phase shift will be π or $\pi/2$, depending on the sensor configuration in the head, and the image in the XY system will be a straight section for $\varphi = \pi$ and a circle for $\varphi = \pi/2$ (Table 2). When the head has a pair of sensors with a shift by π, the components resulting from the shaft face non-perpendicularity errors or shaft bending can be eliminated mathematically by summing both signals and dividing by 2.

For the machine set with a piston machine, specific planes perpendicular to the machine set rotor axis are the plane of the thrust or locating bearing flange and the face of the free end of the shaft. The value of the displacement of axial vibration of the free end face of the machine set rotor shaft is, inter alia, affected by:

- vibration dependent on the rotor alignment (values of cranks deflection);
- vibration as the result of rotor displacement in the axial bearing clearance.

Axial vibration of the crankshaft free end face was tested, with the shaft mounted on a large lathe. The crankshaft flange on the flywheel side was connected with the flange of the lathe spindle. The lathe spindle axial motion was blocked. The main journals of the crankshaft were supported on rollers. The position of the rollers could be altered vertically and horizontally, which enabled forcing crank deflections, leading to forced axial displacements of the shaft free end. The head with sensors was mounted to the tailstock, so the distance between the shaft end and the head could be changed.

The tests made use of the head with a pair of sensors with shift by π and a pair of sensors with shift by $\pi/2$ for various shaft deflections. Some of the test results are shown in Figures 15–18.
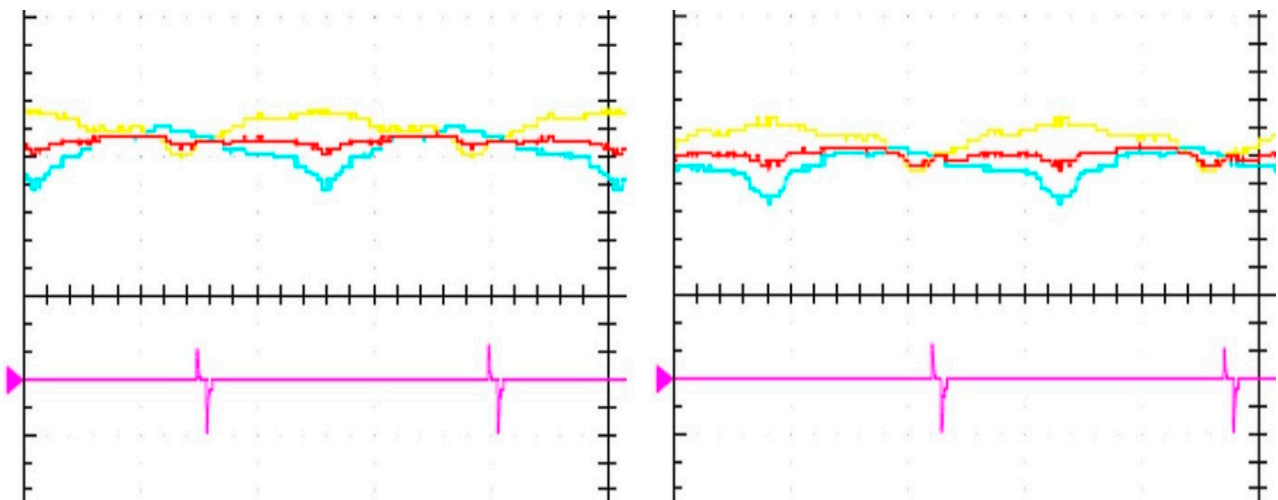

Figure 15. Signals from a pair of sensors with shift by π: on the left—for deflection $\{\Delta_{v1} = (+)0.04; \Delta_{v2} = (+)0.02; \Delta_{v3} = 0.00\}$; on the right—for deflection $\{\Delta_{v1} = (+)0.01; \Delta_{v2} = (-)0.015; \Delta_{v3} = (-)0.005\}$; yellow—signal of sensor CH1, blue—signal of sensor CH2, red—averaged signal (CH1 + CH2)/2, purple—signal of rotation angle marker, blue arrow—zero value of signals (CH1 = 0, CH2 = 0, (CH1 + CH2)/2 = 0). CH1 = CH2 = 1.00 V/DIV; CH1 + CH2 = 2.00 V/DIV.
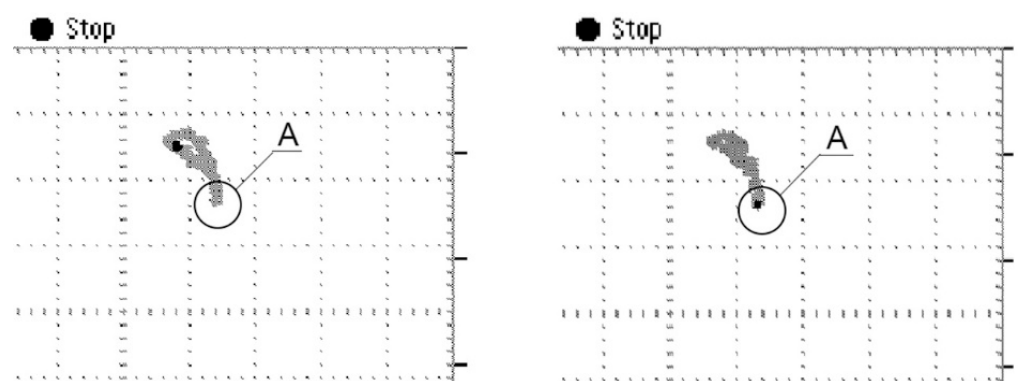

Figure 16. The figures from a pair of sensors with shift by π: left—for deflection $\{\Delta_{v1} = (+)0.04; \Delta_{v2} = (+)0.02; \Delta_{v3} = 0.00\}$, right—for deflection $\{\Delta_{v1} = (+)0.01; \Delta_{v2} = (-)0.015; \Delta_{v3} = (-)0.005\}$. The zero value CH1 = CH1 = (–)9 DIV= (–)4.5 V; CH1 = CH2 = 0.5 V/DIV; A—fragments caused by local inhomogeneity of the material.
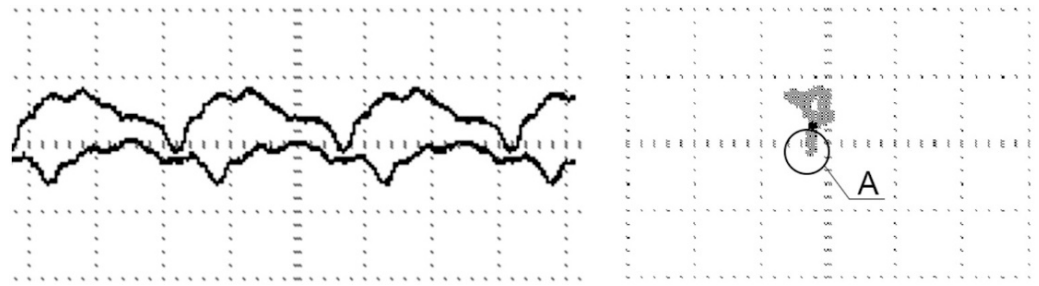
Figure 17. The signals (**left**) and the figure (**right**) from a pair of sensors with shift by $\pi/2$ for deflection $\{\Delta_1 = 0.00; \Delta_2 = -0.03; \Delta_3 = -0.015\}$: A—fragments caused by local inhomogeneity of the material.
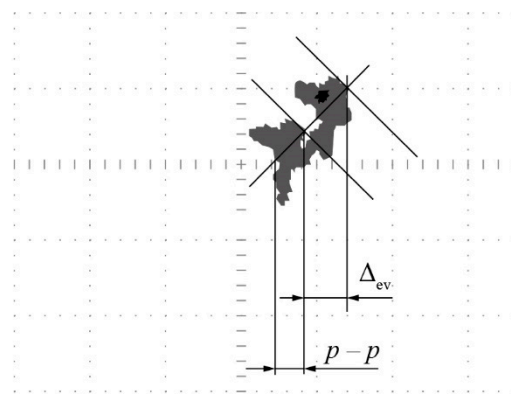

Figure 18. Figures of a pair of sensors with shift by $\pi/2$ at deflection $\{\Delta_1 = 0.00; \Delta_2 = -0.035; \Delta_3 = -0.015\}$ before and after increasing the head–shaft distance by 0.09 mm: CH1 = CH2 = 500 mV/DIV, Δ_{ev}—change of the average value, $|p - p|$—maximum value of the elliptical part of the figure.

It was found that minor changes in crank deflection resulted in measurable changes in axial vibration of the shaft free end. These changes are visible in the time waveforms of sensor signals and in images in the XY system (Figures 17 and 18).

The signal of axial vibration from each sensor is the sum of real axial vibration and the runout signal. The runout signal is created due to errors, such as non-perpendicularity of shaft face, shape and inhomogeneity of material structure of the shaft end face. It follows from Figure 17 that summing of the signals from a pair of sensors with shift by π eliminates the components caused by non-perpendicularity of the end face relative to the shaft rotation axis. The average value, amplitude and phase shift of the averaged signal depend on shaft deflection.

A limited area with different material structure was identified on the shaft end face surface, resulting in the generation of pulse signal components in the time waveform and "tails" in the XY system image, depicted as A in Figures 16 and 17.

It follows from Figures 16–18 that the maximum value $|p - p|$ of the diagonal of the figure depends on shaft deflection. For a pair of sensors with a shift by $\pi/2$, the figure model is an ellipse, and the measure of axial vibration value is the difference between the value of greater and smaller diameters. It also follows from Figure 18 that the change of distance between the head and the shaft face results in a shift of the figure, as the average/constant value Δ_{ev} of axial vibration changes.

5. The Position Head of Marine Engine Crankshaft

At the flywheel end, the crankshaft of a large combustion engine is equipped with a flywheel bearing, sealing of the crankcase and a split gear wheel for camshaft driving. The flywheel bearing can be composed of two radial bearings, of which one is additionally

equipped with a locating bearing or may consist of two radial bearings and a thrust bearing (Figure 19) [23,44,59,60].
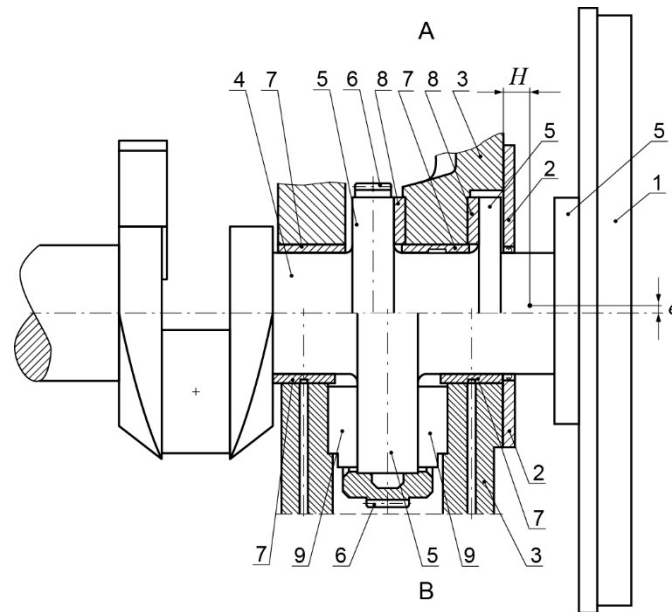

Figure 19. The flywheel end of the crankshaft of engine with locating bearing (part A) and thrust bearing (part B): 1—flywheel, 2—engine cover with sealing, 3—engine body, 4—main journal of shaft, 5—flange of crankshaft, 6—gear wheel for camshaft drive, 7—main bearing shell, 8—thrusting half, 9—thrust pads, H—distance between the face plane of machine body and a point on the crankshaft axis in the measuring plane, *e*—distance between shaft axis and axis of holes in the machine body.

The point located on the journal axis on the flywheel side is to be considered as the point determining the position of the shaft relative to the engine body. The position of the bearing journal center on the flywheel side:

- affects the axial vibration of the crankshaft free end;
- depends on the alignment of the machine set rotor.

The fragment of the engine journal, accessible from the outside, is a fragment between the body and the flywheel. The intersection of the plane parallel to the face of the engine body with shaft and bearing hole axes determines a point on the shaft axis (the journal center) and a point on the bearing hole axis (the bearing center). For the defined plane parallel to the engine body face, the shaft position measurement will consist of the measurement of the journal eccentricity e of the journal in the shell and distance l of the shaft journal center from the face of the engine body (Figure 19). The surface parallel to the engine body face associated with the crankshaft can be the frontal surface of the shaft flange, flywheel or a special ring mounted on the shaft flange. The measurement of the running engine shaft position comes down to the measurement of relative radial and axial vibration of the shaft journal and flange on the flywheel side. The following design solution referred to as the "shaft position head" is proposed for vibration measurements. The head 10 (Figure 20) is composed of a holder and two pairs of eddy current sensors, X1Y1 and X2Y2. The head is rigidly fixed to the upper part of the engine body cover 2 on the flywheel side. The pairs of sensors in the head are shifted relative to each other by $\pi/2$ (Figure 20).
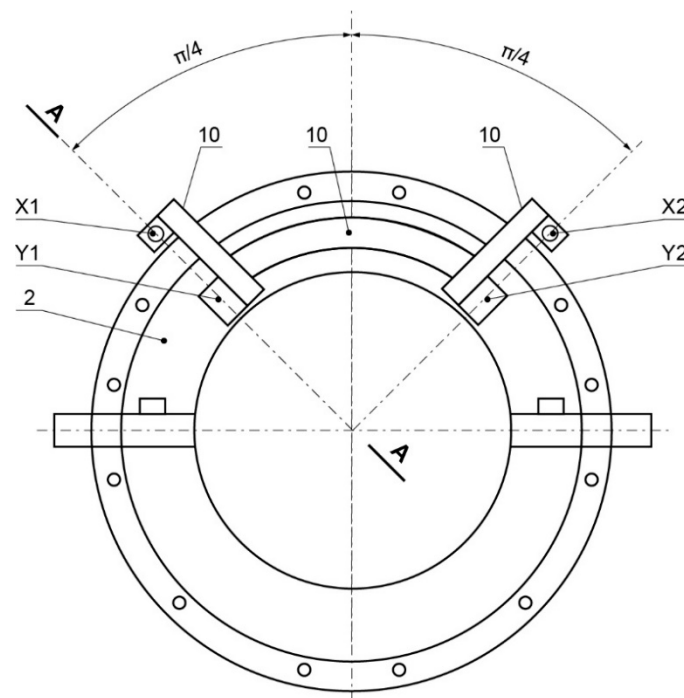
Figure 20. The engine cover with the mounted head: 10—head; 2—engine cover on the flywheel side; X1, X2—sensing element of eddy current sensors for axial measurements; Y1, Y2—sensing element of eddy current sensors for radial measurements.

Sensors X1 and X2 measure the distance between the engine body and the shaft frontal surface. Sensors Y1 and Y2 measure the distance between the body and the shaft cylindrical surface, the shaft flange cylindrical surface or the cylindrical surface of the ring imposed on the flange and connected with the flywheel. The head of a position sensor requires calibration on a special calibration bushing.

The calibration bushing 11 (Figure 21) has a flange for mounting the cover 2 with the head 10, the part with a cylindrical measuring surface and a second flange with a frontal measuring surface. The flange has bolt holes of the same characteristics as bolt holes in the body. These bolt holes are located so that the calibration bushing axis overlaps with the cover axis and, consequently, with the axis of holes for shaft bearings in the machine body. The cylindrical surface is the surface of a cylinder with a diameter d equal to that of the shaft, shaft flange or the external diameter of the mounted ring. The frontal measurement surface of the second flange of the calibration bushing is perpendicular to the bushing axis, placed away from the internal surface of the first flange, at a distance l_0. The distance l_0 is determined by Equation (15).

$$l_0 = (l_{max} - l_{min})/2 \tag{16}$$

where

l_{max}—distance between the machine body and the measurement plane (frontal measuring surface) at the displacement of the crankshaft toward the flywheel,

l_{min}—distance between the machine body and the measurement plane (frontal measuring surface) at the displacement of the crankshaft toward the free end.

The upper cover with the position head is mounted on the calibration bushing; the sensing elements of the sensors are set in the center of the measurement range; the sensing elements of the sensors in the head are blocked, and their indications are recorded. After calibration, the cover with the head is mounted to the machine body. The shape and dimensions of the head and the calibrating bushing dimensions are designed for a given engine.
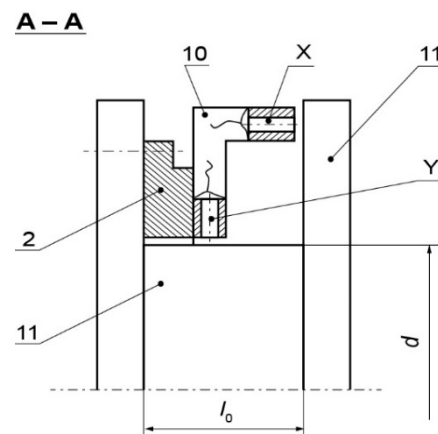
Figure 21. Configuration for calibrating the position head: 2—engine cover; 10—position head; 11—calibration bushing; *d*—diameter of calibration bushing equal to diameter of new shaft in the measurement plane; l_0—distance between internal frontal surfaces of calibrating bushing flanges.

6. The Arrangement of Sensor Heads for Vibration Diagnostics of Marine Propulsion System Rotors

The screw propeller propulsion is the basic propulsion of the ship. In the traditional propulsion systems placed in the hull, the ship's propeller fixed on the shaft converts the energy of the rotary motion into the energy of the thrust on the ship hull. The shaft bearing located in the ship's stern frame called stern tube bearing is a non-split bearing and is fitted with sealings. The effective moment on the propeller and the thrust force generated by the propeller are not constant because the propeller rotates perpendicularly in a non-uniform water stream, resulting from the asymmetry of the ship hull and other protrusions in the vicinity of the propeller's flow field. The main component of axial forces has a frequency known as the blade passing frequency (BPF), which is equal to the shaft rotational frequency multiplied by the number of blades of the propeller and an integer representing the order of BPF [61].

To enhance the ship's safety and the dependability of the propulsion system, the methods of calculating torsional vibration [62] and methods of optimal shafting arrangement [63] are improved, and propeller shafts, shaft bearings and the propeller are subject to technical supervision and periodical surveys [64,65].

The propeller, propeller shaft, bearings and sealings are affected by unavoidable wear, which may be accelerated due to additional events. Damage to the stern bearing is largely a result of bearing displacement due to hull deformation caused by ship loading condition and sea waves.

The most common line is the diesel engine propulsion line with or without gear. The diesel engine propulsion line without a gear has one rotor of the machine set, and the thrust bearing is set in the engine. The diesel engine propulsion line with a gear has two rotors of the machine set; the thrust bearing is usually placed in the gear, and the engine contains a locating bearing. The engine's crankshaft has two ends: the free end and the flywheel end. The engine body on the free end side is often closed with a cover. After removing the cover, the frontal surface of the crank shaft free end is accessible despite the possible presence of a gear for driving pumps and a vibration damper. Similarly, in the case of a gear connected with a fixed pitch propeller, the removal of the gear end cover gives access to the gear shaft end frontal surface. The herein proposed system for diagnosing propulsion systems with combustion engines includes an arrangement of sensor heads, as shown in Figure 22.
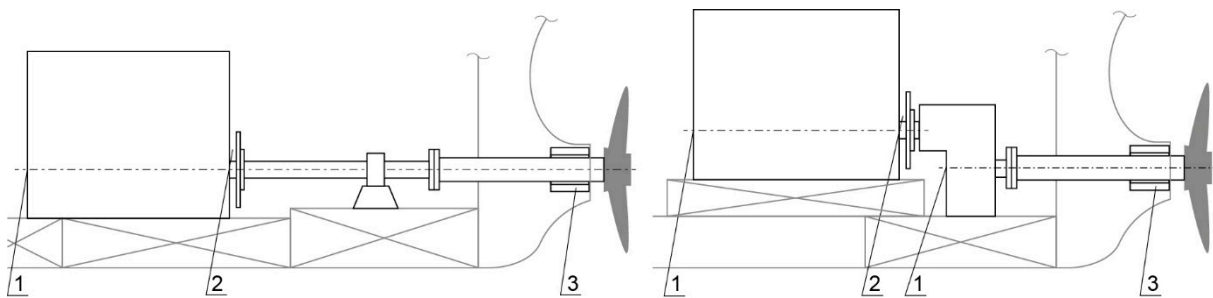
Figure 22. The arrangement of sensor heads for diagnosing diesel engine propulsion lines: 1—head of shaft free end sensors, 2—head of shaft position sensors, 3—head of stern bearing sensors.

In the case of diesel engine propulsion lines without a reduction gear, radial vibration from heads 2 and 3 depends on the wear margin of the bearings, deformations of the hull and machine support. Additionally, the radial vibration from head 3 is dependent on the propeller wear margin. The axial vibration from heads 1 and 2 depends, inter alia, on the wear margin of the main radial bearings of the engine, the thrust bearing and the propeller. The torsional vibration from head 1 depends on the moments acting on the machine set rotor (driving engine, friction moments of all component machines and the effective moment on the propeller), rotor wear margin (shaft cracks, loosened press fits, coupling damage, etc.), wear margin of bearings located in the nodes of torsional vibration, wear margin of torsional vibration damper, etc.

In the case of diesel engine propulsion lines with a reduction gear, the head 1 of free end sensors can be used as the head of the gear shaft free end and with the head 3 of the stern bearing sensors can serve for diagnosing the wear margin of the propeller shaft, the propeller and the thrust bearing. Where the free end of the gear shaft is not accessible, it is possible to use the shaft position head 2 as the head of the propeller shaft position, and with the sensors head 3 of the stern bearing, it may be used for limited diagnostic inference related to the wear margin of the gear–propeller rotor.

The free end head in the form as described in Ref [55] can be installed on machines (including engines) where the free end can be directly accessed. The position head in the proposed solution can be used on engines and other machines, e.g., transmission shafts with a thrust bearing. The head in the solution described in Ref [58] is intended for diagnosis of sleeve bearings.

7. Discussion

The author's approach to machine diagnostics is characterized by the following:

- the machine set is considered,
- the machine set rotor is distinguished as a functional unit,
- the physical models of the relationship between the wear margin measures and the symptoms measures of the machine set rotor are built.

The author's approach differs from the approach found in the literature in the diagnosed objects and/or the model building algorithm. The literature refers to the condition monitoring or fault diagnosis of specific machines or machine systems, e.g., wind turbines [66], combustion engines [67], ship's propeller shaft [68], etc. In the fault diagnostic, the relationships between faults and symptoms are built by means of a computer method, e.g., neural network [4]. In the process of creating relationships, the symptoms and the measures of symptoms are selected arbitrarily, and the damage is defined freely. Condition monitoring is the process of tracking a developing fault; the fault is the result of wear. According to Ref. [69], condition monitoring is justified in cases where it is technically possible to measure the wear of the device element and where the amount of wear changes along with the time of use.

The features describing the wear margin of the machine set rotor are features belonging to the hierarchical feature system; the feature system is described in Ref. [10]. The overriding

feature is the efficiency, which consists of mechanical efficiency of the machine set. The mechanical efficiency of the machine set is essential in enterprise asset management. The goals and tasks of enterprise asset management are described, for example, in Ref. [70].

The features of the lower order are assembly quality features. The quality of the assembly of the machine set rotor consists of clearances and misalignments, whose measured values can be identified on an out-of-operation machine set. The measures and methods of their measurement are described in Refs. [27–30]. The hierarchical setting of the features that make up the wear margin facilitates diagnostic inference and performance of maintenance works. Some authors consider the examination of non-working machines as diagnosis (endoscopy, alignment of coupled machine shafts) or examination identifying the balance of the rotor in machine bearings.

Relative vibration of the rotor shaft as a symptom is used in many systems [23]. In the case of the journal center trajectory, variable components are measured [9]. In this paper, all kinds of relative vibrations of the driving machine–driven machine rotor are comprehensively used as symptoms. Both constant values and variables of symptom measures are measured. Such measurements require solving the problem of "sensor ran out", the influence of other kinds of vibrations on the measured value and sensor calibration. The problem of "sensor ran out" and the influence of other vibrations on the measured vibrations was solved not by acting on the sensor signals as in Ref. [55] but by using more than one axial vibration sensor and additional equipment for the mounting of sensors and sensor calibration equipment. It was shown that in the case of torsional vibrations, synchronous averaging allows separating the vibrations of a given machine set rotor from another machine set rotor.

The torsional vibration angular acceleration $\ddot{\alpha}$ as a function of the rotation angle can be measured at the free end of the rotor shaft. It is recommended to perform the measurement of torsional vibration and free end axial vibration by the sensors head equipped with a non-contact Ferraris sensor, eddy current sensors and key phasor with a converter. Sensors heads of the rotor shaft free end and radial slide bearing are presented in Ref. [52]. The novelty of this paper is also the rotor position head. For a machine set where one machine is a piston machine, it is justified and possible to construct rotor position heads. The position head allows simultaneous measurement of relative radial and axial vibration of the journal center in the flywheel bearing.

The solutions presented in this article are utilitarian. They can be used in various design solutions of machine sets. An example of machine set rotors are rotors of the marine propulsion system. For the rotor of the ship's propulsion system with a combustion engine, a crankshaft free end head can be constructed, as well as a rotor position head and a sleeve stern bearing head. These heads are components of the head arrangement on which a new diagnostic system can be built.

8. Conclusions

1. From the point of view of maintenance, it is justified and technically possible to distinguish the "machine set rotor" as a functional unit in the driving machine–driven machine set found in production and propulsion systems. It is possible to create the model of a machine set rotor.
2. Friction moment can be considered as one of the substitute wear margin measures of the machine set. Changes in the friction moment result in measurable changes in the rotor torsional vibration acceleration.
3. It is possible to identify (substitute) wear margin qualities in the driving machine–driven machine set. The qualities describing the wear margin of the machine set rotor should include alignment, unbalance and transfer function of the machine set rotor. In a machine set rotor supported by slide bearings, the machine set rotor alignment and unbalance have an impact on the value of the position of the journal relative to the shell in the case of radial bearings and the position of the shaft flange relative to the axial bearing shell. The position of the journal and the position of the flange relative to

the corresponding shells also depend on the wear margin of the given bearing, which means that the wear margin of the bearings affects the alignment of the machine set rotor. If the machine set rotor has a crankshaft, the deflection of shaft cranks is a measure of crank alignment. The deflection of cranks causes axial displacement of the crankshaft end frontal surface during the rotation. The (substitute) wear margin measures of the machine set rotor can change in the measure of journal or flange position relative to the corresponding shells and measures of cranks deflection or measure of axial displacement of crankshaft free end.

4. It is possible to identify the (substitute) wear margin measure of the radial and axial slide bearing. They are (for the radial slide bearings) the dimensionless Sommerfeld number and (for axial slide bearings) the bearing load capacity (the number B_k). For radial bearings—the eccentricity of the journal in the shell, while for axial bearings—the distance between the shell and the flange can be used as wear margin symptoms.

5. During the machine set operation, changes in the crank deflection cause measurable changes in the axial vibration of the free end of the crankshaft. Changes in the eccentricity of the radial bearing cause measurable changes in the radial rotor vibration measure, and changes in the distance in axial bearing result in measurable changes in the axial rotor vibration measure.

6. The desired measures of axial vibration of the free crankshaft end are an average value, amplitude and phase shift of the displacement waveform. Because the average value of the displacement of the free end is affected by the displacement of the whole rotor within the axial bearing clearance, simultaneous measurement of the average value of axial displacements in the axial bearing is required.

7. The radial vibration in radial bearing can be measured as the trajectory of the journal center. The desired measures of radial rotor vibration are a distance between the average value of the journal center trajectory and the center of the hole for the bearing shell. The distance can by measured by means of a calibrated sensor head.

8. The desired measures of rotor axial vibration are an average value of the rotor vibration displacement measured in the thrust or the position bearing by means of a calibrated sensor head.

9. For a machine set rotor with crankshaft supported by slide bearings, it is justified and possible to build a position head of the machine set rotor and to find a method of position head calibration.

10. Free crankshaft end head, i.e., the free end head with a Ferraris sensor, displacement sensor and shaft angle sensor with a converter can be used to measure the synchronously averaged waveform and spectrum of the machine set rotor torsional vibration acceleration and axial vibration displacement.

11. The arrangement of the free crankshaft end head, rotor position head and sleeve bearing head should be considered as part of the new diagnostic system for identifying probable causes of wear margin loss of the machine set rotor regarded as a functional unit of the ship's propulsion system.

Institutional Review Board Statement: Not applicable.

Informed Consent Statement: Not applicable.

Data Availability Statement: Not applicable.

Conflicts of Interest: The author declares no conflict of interest.

References

1. Trianni, A.; Cagno, E.; Bertolotti, M.; Thollander, P.; Andersson, E. Energy management: A practice-based assessment model. *Appl. Energy* **2019**, *235*, 1614–1636. [CrossRef]
2. Shang, Z.; Gao, D.; Jiang, Z.; Lu, Y. Towards less energy intensive heavy-duty machine tools: Power consumption characteristics and energy-saving strategies. *Energy* **2019**, *178*, 263–276. [CrossRef]
3. Timashev, S.; Bushinskaya, A. *Diagnostics and Reliability of Pipeline Systems*; Springer: Cham, Switzerland, 2016.
4. Vijayalakshmia, S.; Karthikhab, R.; Paramasivamc, A.; Bhaskar, K.B. Condition Monitoring of Industrial Motors using Machine Learning Classifiers. In Proceedings of the International Conference on IoT based Control Networks and Intelligent Systems (ICICNIS 2020), Kerala, India, 10–11 December 2020.
5. Jin Guo, J.; Liu, Y.; Li, K.; Liu, Q. Research on an ID-PCA Early Fault Detection Method for Rolling Bearings. *Appl. Sci.* **2022**, *12*, 4267.
6. Del Buono, F.; Calabrese, F.; Baraldi, A.; Paganelli, M.; Guerra, F. Novelty Detection with Autoencoders for System Health Monitoring in Industrial Environments. *Appl. Sci.* **2022**, *12*, 4931. [CrossRef]
7. *ISO 17359:2018*; Condition Monitoring and Diagnostics of Machines—General Guidelines. International Organization for Standardization: Geneva, Switzerland, 2018; p. 1.
8. *ISO 7919-1:1996(en)*; Mechanical Vibration of Non-Reciprocating Machines—Measurements on Rotating Shafts and Evaluation Criteria—Part 1: General Guidelines. International Organization for Standardization: Geneva, Switzerland, 1996.
9. *ISO10816-1:1995/Amd.1:2009(en)*; Mechanical Vibration—Evaluation of Machine Vibration by Measurements on Non-Rotating Parts—Part 1: General Guidelines Amendment 1. International Organization for Standardization: Geneva, Switzerland, 2009.
10. Bielawski, P. Miary i wartości graniczne potencjału eksploatacyjnego maszyn systemów produkcyjnych/Measures and limits of machine wear margin of production systems. *Probl. Eksploat. Maint. Probl.* **2016**, *1*, 129–159.
11. Bielawski, P. Identification of the Wear Margin of a Pipeline—Machine Subsystem. *Appl. Sci.* **2020**, *10*, 3977. [CrossRef]
12. Fehrenbach, H.; Quante, F.; Besserdich, G. Diagnosis of Combustion Engines by the Analysis of the Crankshaft's Rorational Speed. *VDI Ber.* **1987**, *644*, 73–80.
13. Biezeno, C.B.; Grammel, R. *Technische Dynamik*; Band 2; Springer: Berlin/Heidelberg, Germany; New York, NY, USA, 1953.
14. Trybuła, W. *Ocena Stanu Technicznego Silnika Spalinowego Metodą Przyspieszeń. Diagnostyka Pojazdów*; Ossolineum: Wrocław, Poland, 1981; pp. 75–92.
15. Arkuszewski, A.; Wdowiak, W. Wpływ Niedomagań Silnika z Zapłonem Samoczynnym na Charakterystykę Bezwładnościową—Źródło Informacji Diagnostycznych. Ph.D. Thesis, Politechnika Poznańska, Poznań, Poland, 1983.
16. Jankowski, M.; Żółtowski, B. Komputerowa kontrola efektywności pracy silnika spalinowego metodą przyspieszeń. *Zagadnienia Eksploat. Masz.* **1993**, *4*, 541–551.
17. Piętek, A. *Charakterystyki Dynamiczne Silników o Zapłonie Samoczynnym i Ich Aplikacje Diagnostyczne*; WAT: Warszawa, Poland, 1997.
18. Wang, A.; Luo, Z. Performance Degradation Research of Combined Rotor Considering Rod Relaxation. In Proceedings of the 3rd International Conference on Materials Engineering, Manufacturing Technology and Control (ICMEMTC 2016), Taiyuan, China, 27–28 February 2016; pp. 911–917.
19. Murawski, L. Shaft line alignment analysis taking ship construction flexibility and deformations into consideration. *Mar. Struct.* **2005**, *18*, 62–84. [CrossRef]
20. *ISO 1940-1*; Mechanical Vibration—Balance Quality Requirements for Rotor in a Constant (Rigid) State, Part 1: Specification and Verification of Balance Tolerances. International Organization for Standardization: Geneva, Switzerland, 2003.
21. Uhl, T.; Lisowski, W. *Praktyczne Problemy Analizy Modalnej Konstrukcji*; AGH: Kraków, Poland, 1996.
22. Kolerus, J.; Wassermann, J. *Zustandsüberwachung von Maschinen*; Expert Verlag: Renningen, Germany, 2008.
23. Klein, U. *Schwingungsdiagnostische Beurteilung von Maschinen und Anlagen*; Verlag Stahleisen GmbH: Düsseldorf, Germany, 2000.
24. Goldman, S. *Vibration Spectrum Analysis: A Practical Approach*; Industrial Press Inc.: New York, NY, USA, 1999.
25. Nowikow, M.P. *Podstawy Technologii Montażu Maszyn I Mechanizmów*; WNT: Warszawa, Poland, 1972.
26. Bielawski, P. *Identyfikacja Obiektów Technicznych Systemów Produkcyjnych*; Akademia Morska w Szczecinie: Szczecin, Poland, 2014.
27. *Machine Diagnosis, Field Balancing, Shaft Alignment: Methods, Benefits and Solutions*; Seminar C44; Carl Schenck AG: Darmstadt, Germany, 1995.
28. Morel, J. *Drgania Maszyn I Diagnostyka Ich Stanu Technicznego*; Wyd. Polskie Towarzystwo Diagnostyki Technicznej: Warszawa, Poland, 1992.
29. *Wärtsilä 64 Instruction Manual*; Wärtsilä NSD Italia S.p.A.: Trieste, Italy, 1999.
30. Meier-Peter, H. Das Ausrichten von Schiffswellenleitungen. *Hansa* **1985**, *4*, 351–353.
31. Zhang, Y.; Biboulet, N.; Venner, C.H.; Lubrecht, A.A. Prediction of the Stribeck Curve under full-film Elastohydrodynamic Lubrication. *Tribol. Int.* **2020**, *149*, 105569. [CrossRef]
32. Böswirth, L.; Bschorer, S. *Technische Strömungslehre*; Vieweg + Teubner Verlag: Wiesbaden, Germany, 2012.
33. Neale, M.J. *The Tribology Handbook*; Butterworth-Heinemann: Oxford, UK, 1995.
34. Hebda, M.; Wachal, A. *Trybologia*; WNT: Warszawa, Poland, 1980.
35. Krzemiński-Freda, H. *Łożyska Toczne*; PWN: Warszawa, Poland, 1985.
36. Barwell, F.T. *Łożyskowanie*; WNT: Warszawa, Poland, 1984.
37. *VDI 2204*; Verein Deutscher Ingenieure. Verein Deutscher Ingenieure: Düsseldorf, Germany, 1992.

38. Spiegel, K.; Fricke, J. Bemessungs-und Gestaltungsregeln für Gleitlager: Herkunft-Bedeutung-Grundlagen-Fortschritt. *Tribol. Schmier.* **2000**, *47*, 32–41.

39. Spiegel, K.; Fricke, J. Bemessungs-und Gestaltungsregeln für Gleitlager: Optimierungsfragen. *Tribol. Schmier.* **2003**, *50*, 5–14.

40. Spiegel, K.; Fricke, J. Bemessungs-und Gestaltungsregeln für Gleitlager: Anlagewinkel, An- und Auslauf, Beanspruchung der Gleitflächen. *Tribol. Schmier.* **2007**, *54*, 5–17.

41. Spiegel, K.; Fricke, J. Bemessungs-und Gestaltungsregeln für Gleitlager: Turbulenz und Instabilitäten. *Tribol. Schmier.* **2008**, *55*, 16–24.

42. *DIN 31653*; Gleitlager. Hydrodynamische Axial-Gleitlager im Stationären Betrieb. Berechnung von Axialsegmentlagern (Plain Bearings; Hydrodynamic Plain Thrust Bearings under Steady-State Conditions; Calculation of Pad Thrust Bearings). Deutche Institut für Normung e.V.: Berlin, Germany, 1991.

43. *Wärtsilä 32 Spare Parts Catalogue*; Wärtsilä Finland OY: Vaasa, Finland, 2006.

44. Kozłowiecki, H. *Łożyska Tłokowych Silników Spalinowych*; WKiŁ: Warszawa, Poland, 1974.

45. *DIN 31652*; Hydrodynamische Radial-Gleitlager im stationären Bereich. Deutche Institut für Normung e.V.: Berlin, Germany, 2017.

46. Bielawski, P. Measures and symptoms of wear margin in functional unit nodes of production system items. *J. Mach. Constr. Maint. Probl. Eksploat.* **2017**, *3*, 117–126.

47. Bielawski, P. *Elementy Diagnostyki Mechanizmów Tłokowo-Korbowych Maszyn Okrętowych*; Studia 39; WSM: Szczecin, Poland, 2002.

48. Bielawski, P. The Diagnosing of Crankshafts. In Proceedings of the 18th International Congress and Exhibition on Condition Monitoring and Diagnostic Engineering Management (COMADEM 2005), Cranfield, UK, 31 August–2 September 2005; pp. 131–142.

49. Deutch, G. Maschinenüberwchung. Schwingungsüberwachung und–diagnose. *Tribol. Schmier.* **2009**, *56*, 39–46.

50. Schrüfer, E. *Elektrische Messtechnik*; Carl Hanser Verlag: München, Germany; Wien, Austria, 2004.

51. Bielawski, P. Marine Propulsion System Vibration Sensor Heads. *New Trends Prod. Eng.* **2018**, *1*, 729–737. [CrossRef]

52. Ellin, A.; Dolsak, G. The design and application of rotary encoders. *Sens. Rev.* **2008**, *28*, 150–158. [CrossRef]

53. Hiller, B. Ferraris Acceleration Sensor—Principle and Field of Application in Servo Drives. Available online: https://pl.scribd.com/document/81194247/Ferraris-Acceleration-Sensor (accessed on 10 January 2018).

54. Faßnacht, J.; Mutschler, P. An Observer to Improve the Speed Signal Using a Ferraris Acceleration Sensor. Available online: https://www.lea.tu-darmstadt.de/media/srt/medien/forschung_5/jf_epe01.pdf (accessed on 6 January 2021).

55. Zintegrowana Głowica Pomiarowa, Zwłaszcza do Badań Drgań Wolnego Końca Wału Maszyn. PL Patent 231,789, 27 December 2016.

56. Tkotz, K. (Ed.) *Fachkunde Elektrotechnik*; Verlag Europa-Lehrmittel: Haan-Gruiten, Germany, 2005.

57. Rybczyński, J. Estimation of dynamic condition of rotating machine of the ground of trajectories of bearing journals. *Tribologia* **2002**, *2*, 661–676. (In Polish)

58. Sposób Wzorcowania Układu Sensorów do Pomiaru Mimośrodowości Wirującego Wału Zwłaszcza Wału Łożyska Ślizgowego z Uszczelnieniem Promieniowym. PL Patent 233,403, 7 December 2017.

59. *MAN L40/45*; Spare Parts Catalogue. M.A.N.: Augsburg, Germany, 1980.

60. *Service Instructions for Sulzer Diesel Engine RTA72U*; New Sulzer Diesel Ltd.: Winterthur, Switzerland, 1993.

61. Youssef, A.; Matthews, D.; Guzzomi, A.; Pan, J. Contact Force Measurement in an Operational Thrust Bearing using PVDT Film at the Blade and Pad Passing Frequencies. *Sensors* **2018**, *18*, 3956. [CrossRef] [PubMed]

62. Senjanović, I.; Ančić, I.; Magazinović, G.; Alujević, N.; Vladimir, N.; Cho, D.-S. Validation of analytical methods for the estimation of the torsional vibrations of ship power transmission systems. *Ocean. Eng.* **2019**, *184*, 107–120. [CrossRef]

63. Kim, Y.-G.; Kim, U.-K. Design and analysis of the propulsion shafting system in a ship with single stern tube bearing. *J. Mar. Sci. Technol.* **2020**, *25*, 536–548. [CrossRef]

64. Polski Rejestr Statków. *Przepisy Klasyfikacji i Budowy Statków Morskich*; Polski Rejestr Statków: Gdańsk, Poland, 2017.

65. Polski Rejestr Statków. *Przeglądy Okresowe Wałów Śrubowych*; Publikacja Nr 111/P; Polski Rejestr Statków: Gdańsk, Poland, 2017.

66. Fischer, K.; Coronado, D. Condition monitoring of wind turbines: State of the art, user experience and recommendations—VGB Research Project 383. *VGB Power Tech* **2015**, *7*, 51–56.

67. Jukl, M.; Polcar, A.; Čupera, J. Possibilities of monitoring the technical condition of combustion engine with starter load current. *Acta Univ. Agric. Silvic. Mendel. Brun.* **2014**, *62*, 961–969. [CrossRef]

68. Yang, K.; Zhou, X.; Liao, S.; Li, L.; Qin, L. Design of a Non-Contact Condition Monitoring System for the Fault Diagnosis of Shaft in Marine Propulsion System. *Open Mech. Eng. J.* **2012**, *6*, 155–161. [CrossRef]

69. *VDI 2888*; 1999 Maintenance Condition Monitoring. Verlag des Vereins Deutscher Ingenieure: Düsseldorf, Germany, 1999.

70. Mann, A. *Enterprise Asset Management Overview*; Helber Hastert & Fee Planners Inc.: Honolulu, HI, USA, 2017.